Symmetries, stability, and control in nonlinear systems and networks

Giovanni Russo[1,*] and Jean-Jacques E. Slotine[2,†]
[1]*Department of Systems and Computer Engineering, University of Naples Federico II, Italy*
[2]*Nonlinear Systems Laboratory, Massachusetts Institute of Technology, Cambridge, Massachusetts, USA*
(Received 31 October 2010; revised manuscript received 29 August 2011; published 24 October 2011)

This paper discusses the interplay of symmetries and stability in the analysis and control of nonlinear dynamical systems and networks. Specifically, it combines standard results on symmetries and equivariance with recent convergence analysis tools based on nonlinear contraction theory and virtual dynamical systems. This synergy between structural properties (symmetries) and convergence properties (contraction) is illustrated in the contexts of network motifs arising, for example, in genetic networks, from invariance to environmental symmetries, and from imposing different patterns of synchrony in a network.

DOI: 10.1103/PhysRevE.84.041929 PACS number(s): 87.10.−e, 05.45.−a, 89.75.Kd

I. INTRODUCTION

Symmetry is a fundamental topic in many areas of physics and mathematics [1–3]. Many systems in nature and technology possess some symmetry, which somehow influences their functionality. Taking into account such a property may significantly simplify the study of a system of interest. In dynamical systems [1], symmetry concepts have been used, for example, to explain the onset on instability in feedback systems [4], to design observers [5] and controllers [6,7], and to analyze synchronization properties and associated symmetry detection mechanisms [8,9]. Typically, the symmetries of a physical system are preserved in the mathematical tools used to model it. This is the case, for instance, of Lagrangian systems, where it can be easily shown that the symmetries of the Lagrangian function transfer onto the equations of motion, making them invariant under the same symmetry (see, e.g., Ref. [6] in the context of motion control).

Our goal in this paper is to develop a theoretical framework to study the rich interplay between symmetries of the system dynamics and questions of stability and control. We make use of the well-known fundamental results introduced in Refs. [1,10–12] and build upon them a theoretical framework for studying the interplay between symmetries of dynamical systems and global stability. The above cited papers were mainly focused on studying symmetry properties of a system of interest and in determining how the possible final behaviors are related to these symmetries and to their bifurcations [13]. Our approach yields global stability and convergence results that can be used to study a large variety of systems, ranging from biochemical network motifs to networked systems. Moreover, these results are further generalized by showing that it is possible to use virtual systems in place of the real systems for performing convergence analysis. These more general virtual systems may have symmetries and convergence properties that the real systems do not.

Stability and convergence analysis is based on nonlinear contraction theory [14,15], a viewpoint on incremental stability that has emerged as a powerful tool in applications ranging from Lagrangian mechanics to network control. Historically, ideas closely related to contraction can be traced back to Ref. [16] and even to Ref. [17]. As pointed out in Ref. [14], contraction is preserved through a large variety of systems combinations, and in particular it represents a natural tool for the study and design of synchronization mechanisms [15]. Here the contraction theory framework also shows that, in fact, for symmetry to play a key role in convergence analysis and control, it needs not be exhibited by the physical system itself but only by a much more general virtual system derived from it. As such, our results provide a systematic framework extending and generalizing the results of Refs. [8,9] in this context.

The paper is organized as follows. After reviewing symmetries and contraction in Secs. II A and II B, some basic results linking the two notions are described in Sec. II C. These results are generalized in Sec. III, where systems with multiple symmetries are considered. Section III B considerably extends the basic results by showing that the contraction and symmetry conditions on the system of interest can be replaced by weaker conditions on some appropriately constructed virtual system. In Sec. IV, the approach is applied to the case of systems with external inputs, with examples detailed in Sec. V. Using our approach we explain the onset of the so-called fold change detection behavior, which is important for biochemical processes. Section VI extends our theoretical framework to the study of interconnected systems or networks, and shows that it can be used to analyze and/or control synchronization patterns. Applications are then provided by showing that symmetries and contraction can be controlled so as to generate different synchronization patterns. Quorum sensing networks are also analyzed. Brief concluding remarks are offered in Sec. VIII.

A. Notation

We denote with $|x|$ any vector norm of the vector $x \in \mathbb{R}^n$ and with $\|A\|$ the induced matrix norm of the real square matrix $A \in \mathbb{R}^{n\times n}$. When needed, we will point out the particular norm being used by means of subscripts: $|\cdot|_i$, $\|\cdot\|_i$. Given a vector norm on Euclidean space, $|\cdot|$, with its induced matrix norm $\|A\|$, the associated matrix measure μ is defined as the directional derivative of the matrix norm, that is, $\mu(A) = \lim_{h\to 0^+} \frac{1}{h}\left(\|I + hA\| - 1\right)$. The matrix measure, also known as logarithmic norm was introduced in Refs. [18] and [19].

*Also at Massachusetts Institute of Technology, Cambridge, Massachusetts 02139, USA. giovanni.russo2@unina.it
†jjs@mit.edu

TABLE I. Standard matrix measures for a real $n \times n$ matrix, $A = [a_{ij}]$. The ith eigenvalue of A is denoted with $\lambda_i(A)$.

Vector norm $\lvert\cdot\rvert$	Induced matrix measure $\mu(A)$
$\lvert x\rvert_1 = \sum_{j=1}^{n} \lvert x_j\rvert$	$\mu_1(A) = \max_j (a_{jj} + \sum_{i \neq j} \lvert a_{ij}\rvert)$
$\lvert x\rvert_2 = (\sum_{j=1}^{n} \lvert x_j\rvert^2)^{\frac{1}{2}}$	$\mu_2(A) = \max_i [\lambda_i(\frac{A+A^*}{2})]$
$\lvert x\rvert_\infty = \max_{1\leqslant j\leqslant n} \lvert x_j\rvert$	$\mu_\infty(A) = \max_i (a_{ii} + \sum_{j \neq i} \lvert a_{ij}\rvert)$

When needed, we will point out the particular matrix measure being used by means of subscripts. Examples of matrix measures are listed in Table I. More generally, matrix measures can be induced by weighted vector norms $|x|_{\Theta,i} = |\Theta x|_i$, with Θ a constant invertible matrix and $i = 1,2,\infty$. Such measures, denoted with $\mu_{\Theta,i}$, are linked to the standard measures by $\mu_{\Theta,i}(A) = \mu_i(\Theta A \Theta^{-1})\ \forall i = 1,2,\infty$.

II. MATHEMATICAL PRELIMINARIES

A. Contraction theory tools

Consider the m-dimensional deterministic system

$$\dot{x} = f(x,t) \tag{1}$$

where f is a smooth nonlinear function. The following definition will be used in the rest of the paper:

Definition 1. The dynamical system Eq. (1) is said to be contracting if there exists some matrix measure, μ, such that $\exists \lambda > 0, \forall x, \forall t \geqslant 0, \mu(\frac{\partial f(x,t)}{\partial x}) \leqslant -\lambda$. The scalar λ defines the contraction rate of the system.

For convenience, in this paper we will also say that a function $f(x,t)$ is contracting if the system $\dot{x} = f(x,t)$ satisfies the sufficient condition above. Similarly, we will then say that the corresponding Jacobian matrix $\frac{\partial f}{\partial x}(x,t)$ is contracting.

The basic result of nonlinear contraction analysis states that, if a system is contracting, then all of its trajectories converge toward each other (see Ref. [14]).

Theorem 1: Contraction. Let $\bar{x}(t)$ and $\tilde{x}(t)$ be two solutions of Eq. (1), with initial conditions $\bar{x}(t_0) = \bar{x}_0$ and $\tilde{x}(t_0) = \tilde{x}_0$. Then, for any $t \geqslant t_0$, it holds that

$$|\bar{x}(t) - \tilde{x}(t)| \leqslant |\bar{x}_0 - \tilde{x}_0| e^{-\lambda t}.$$

We shall also use the following property of contracting systems, whose proofs can be found in Refs. [14,20].

Hierarchies of contracting systems. Assume that the Jacobian of Eq. (1) is in the form

$$\frac{\partial f}{\partial x}(x,t) = \begin{bmatrix} J_{11} & J_{12} \\ 0 & J_{22} \end{bmatrix} \tag{2}$$

corresponding to a hierarchical dynamic structure. The J_{ii} may be of different dimensions. Then, a sufficient condition for the system to be contracting is that (i) the Jacobians J_{11}, J_{22} are contracting (possibly with different Θ's and for different matrix measures), and (ii) the matrix J_{12} is bounded.

A simple yet powerful extension to nonlinear contraction theory is the concept of partial contraction, which was introduced in Ref. [15].

Theorem 2: Partial contraction. Consider a smooth nonlinear n-dimensional system of the form $\dot{x} = f(x,x,t)$ and assume that the auxiliary system $\dot{y} = f(y,x,t)$ is contracting with respect to y. If a particular solution of the auxiliary y system verifies a smooth specific property, then all trajectories of the original x system verify this property exponentially. The original system is said to be partially contracting.

Indeed, the virtual y system has two particular solutions, namely $y(t) = x(t)$ for all $t \geqslant 0$ and the particular solution with the specific property. Since all trajectories of the y system converge exponentially to a single trajectory, this implies that $x(t)$ verifies the specific property exponentially.

Using the Euclidean norm, the results in Ref. [15] are systematically extended in Ref. [8] to global exponential convergence toward some flow-invariant linear subspace, $\mathcal{M}$, allowing in particular multiple groups of synchronized elements to coexist (so called polydynamics, or polyrhythms). The dynamics in Eq. (1) is said to be contracting toward $\mathcal{M}$ if all its trajectories converge toward $\mathcal{M}$ exponentially. Let p be the dimension of $\mathcal{M}$ and V be a $(n-p) \times n$ matrix, whose rows are an orthonormal basis of $\mathcal{M}^\perp$. The following result is a straightforward generalization of Theorem 1 in Eq. [8].

Theorem 3. If $\mu(V \frac{\partial f}{\partial x} V^T)$ is uniformly negative for some matrix measure μ in $\mathbb{R}^{n-p}$, then Eq. (1) is contracting toward $\mathcal{M}$. Note that if the system is contracting, then trivially it is contracting toward $\mathcal{M}$ (since entire trajectories of the system are contained in $\mathcal{M}$).

B. Symmetry of dynamical systems

In this paper, we consider operators acting over the state space of Eq. (1). Often such operators are linear, with their effects on the structure of the solutions specified in terms of a group of transformations (see, e.g., Ref. [1]). We will use the following standard definitions.

Definition 2. Let Γ be a group of operators acting on $\mathbb{R}^n$. We say that $\gamma \in \Gamma$ is a symmetry of Eq. (1) if for any solution, $x(t)$, $\gamma x(t)$ is also a solution. Furthermore, if $\gamma x = x$, we say that the solution $x(t)$ is γ symmetric.

Definition 3. Let Γ be a group of operators acting on $\mathbb{R}^n$, and $f : \mathbb{R}^n \times \mathbb{R}^+ \to \mathbb{R}^n$. The vector field, f, is said to be Γ equivariant if $f(\gamma x,t) = \gamma f(x,t)$, for any $\gamma \in \Gamma$ and $x \in \mathbb{R}^n$. Thus, Γ equivariance in essence means that γ commutes with f.

Definition 4. We say that a solution of Eq. (1) is h symmetric, if there exists some $T > 0$ such that $x(t) = \gamma x(t+T)$. The vector field, f, is said to be h equivariant if $f(\gamma x,t) = \gamma f(x,t+T)$.

We will refer to γ and h as actions. We remark here that forced systems with a nontrivial h symmetry are periodically forced systems. More precisely, suppose h has order m and

$$f(hx,t) = hf(x,t+T).$$

Then

$$f(x,t) = f(h^m x,t) = h^m f(x,t+mT) = f(x,t+mT),$$

which implies that the forcing is indeed periodic. Moreover, if H is a group of h symmetries, then H/Γ must be a cyclic group. The proof is similar to the one for spatiotemporal symmetries of periodic solutions in Ref. [1].

1. Symmetries, equivariance, and invariant subspaces

We first review the relationship [1] between symmetries, equivariance, and the existence of flow-invariant linear subspace.

If f is Γ equivariant, then γ is a symmetry of Eq. (1). Indeed, letting $y(t) = \gamma x(t)$, we have

$$\dot{y} = \gamma \dot{x} = \gamma f(x,t) = f(\gamma x,t) = f(y,t)$$

so that $y(t)$ is also a solution of Eq. (1).

If the operator γ is linear, this in turn immediately implies that the subspace $\mathcal{M}_\gamma = \{x \in \mathbb{R}^n : \gamma x = x\}$ is flow invariant under the dynamics in Eq. (1). Thus, solutions having symmetric initial conditions, $x_0 = \gamma x_0$, preserve that symmetry for any $t \geqslant 0$. Note that $\mathcal{M} \neq \emptyset$ since $\mathbf{0} \in \mathcal{M}$.

In this paper we assume γ to be any linear operator and give some extensions for nonlinear operators. Therefore, our framework is somewhat broader than that typically considered in the literature on symmetries of dynamical systems, where it is generally assumed that γ describes finite groups or compact Lie groups (see, e.g., Ref. [1] and references therein).

C. Basic results on symmetries and contraction

Next, we review some results from Ref. [9], which this paper shall generalize. These results can be summarized as follows: (i) if the dynamical system of interest is contracting, then γ and h symmetries of the vector fields are transferred onto symmetries of trajectories; (ii) if f presents a spatial symmetry γ, then this property can be transferred to the solutions $x(t)$ by only requiring contraction towards $\mathcal{M}_\gamma$, rather than contraction of the entire system. Note that, although the proofs in Ref. [9] are presented in the context of Euclidean norms, they can be generalized straightforwardly to other norms.

Theorem 4. Consider dynamics in Eq. (1), with f Γ equivariant. Assume that f is also contracting, or more generally that f is contracting toward $\mathcal{M}_\gamma$. Then, any solution of Eq. (1) converges toward a γ-symmetric solution.

Proof. The proof is immediate, since any system trajectory tends exponentially toward $\mathcal{M}$, and by definition $\mathcal{M}_\gamma$ is the subspace $x = \gamma x$. ■

We remark here that Theorem 4 implies that all nontransient dynamics lies (e.g., equilibrium points, periodic and chaotic attractors) in $\mathcal{M}_\gamma$. One interesting interpretation of the above theorem is as follows. Assume that $f(x,t)$ in Eq. (1) is Γ equivariant. We know (see Sec. II B) that if $x(t)$ is a solution of Eq. (1), then so is $\gamma x(t)$, which implies in particular that the subspace $\mathcal{M}_\gamma$ is flow invariant under Eq. (1). Assume now that f is contracting toward $\mathcal{M}_\gamma$. Then, given arbitrary initial conditions in $x(t)$, both $x(t)$ and $\gamma x(t)$ will tend to $\mathcal{M}_\gamma$, and therefore will tend to the same trajectory, since by definition $\mathcal{M}_\gamma = \{x \in \mathbb{R}^n : x = \gamma x\}$. Thus, all trajectories initialized within a group transformation generated by γ represent an equivalence class which will converge to the same trajectory on $\mathcal{M}_\gamma$.

Furthermore, note that adding to the dynamics in Eq. (1) any term $\dot{x}_\mathcal{M}(t) \in \mathcal{M}_\gamma$ preserves contraction to $\mathcal{M}_\gamma$. By choosing $\dot{x}_\mathcal{M}(t)$ to represent a multistable attractor, this property could be used to spread out or separate solutions corresponding to different equivalence classes, in a fashion reminiscent of recent work on image classification [21].

A similar transfer of symmetries of the vector field onto symmetries of x holds for spatiotemporal symmetries. Let p_h be the order of h (i.e., $h^{p_h} =$ identity). The following result holds:

Theorem 5. If f is h equivariant and contracting, then x tends to an h symmetric. Furthermore, all the solutions of the system tend to a periodic solution of period $p_h T$.

Proof. Note first that if $x(t)$ is a solution of Eq. (1), then so is $hx(t-T)$, since

$$\frac{dhx(t+T)}{dt} = h\dot{x}(t+T) = f(hx(t+T),t).$$

Since Eq. (1) is contracting, this implies that $x(t) \rightarrow hx(t-T)$ exponentially. By recursion, $x(t) \rightarrow h^{p_h}x(t+p_hT) = x(t+p_hT)$ exponentially. Now exponential convergence of the above implies implies in turn that for any $t \in [0,p_hT]$, $x(t+np_hT)$ is a Cauchy sequence. Since $\mathbb{R}^n$ (equipped with either of the weighted 1, 2, or ∞ norms) is a complete space, this shows that the limit $\lim_{n\rightarrow+\infty} x(t+np_hT)$ does exist, which completes the proof. ■

Note that p_hT may actually be an integer multiple of the smallest period of the solutions.

III. MULTIPLE SYMMETRIES AND VIRTUAL SYSTEMS

In this section, we start by extending the results presented above by considering the case where f presents more than one symmetry. A further generalization is then given using virtual systems: In this way, our approach is extended to the study of systems that present no symmetries.

A. Coexistence of multiple spatial symmetries

In the preceding section, we showed that the symmetries of the vector field of Eq. (1) are transformed in symmetries of its solutions, $x(t)$, if the system is contracting (toward some linear invariant subspace). We now assume that f is equivariant with respect to a number of $s > 1$ actions: The aim of this section is to provide sufficient conditions determining the final behavior of the system.

Let (i) $\mathcal{M}_i$ be the linear subspace defined by γ_i (i.e., $\mathcal{M}_i = \{x : x = \gamma_i x\}$); (ii) $\dot{x}^i = f^i(x^i,t)$ be the dynamics of Eq. (1) reduced on $\mathcal{M}_i$; and (iii) $\gamma_1,\ldots,\gamma_s$ be the symmetries showed by f^i.

Theorem 6. Assume that $\mathcal{M}_1 \subset \mathcal{M}_2 \subset \cdots \subset \mathcal{M}_s$. Then, all the solutions of Eq. (1) exhibit the symmetry γ_j $(1 \leqslant j \leqslant s)$ if (i) Eq. (1) contracts toward $\mathcal{M}_s$ and (ii) $\forall i = j+1,\ldots,s$, $\dot{x}^i = f^i(x^i,t)$ is contracting toward $\mathcal{M}_{i-1}$.

Proof. By assumption we know that the sets $\mathcal{M}_i$ are all linear invariant subspaces. Denote with λ_i the contraction rates of $\dot{x}^i = f^i(x^i,t)$ toward $\mathcal{M}_{i-1}$. Let $a_i(t)$ be solutions of Eq. (1) such that $a_i(0) \in \mathcal{M}_i$, and let $b(t)$ be a solution of Eq. (1) such that $b(0) \notin \mathcal{M}_s$. We have

$$\begin{aligned}
&|b(t) - a_j(t)| \\
&\quad = \left| b(t) + \sum_{i=j+1}^{s} a_i(t) - \sum_{i=j+1}^{s} a_i(t) - a_j(t) \right| \\
&\quad \leqslant |b(t) - a_s(t)| + \sum_{i=j+1}^{s} |a_i(t) - a_{i-1}(t)|.
\end{aligned}$$

Now, by hypotheses, the dynamics of Eq. (1) reduced on each of the subspaces $\mathcal{M}_i$ $(i = j+1,\dots,s)$ [i.e., $\dot{x}^i = f^i(x^i,t)$] is contracting toward $\mathcal{M}_{i-1}$. Thus, there exists some $K_i > 0$, $i = 1,\dots,j-1$, such that

$$|b(t) - a_s(t)| \leqslant K_{s+1}e^{-\lambda_{s+1}t}$$
$$|a_i(t) - a_{i-1}(t)| \leqslant K_i e^{-\lambda_i t} i = j+1,\dots,s$$

This implies that $\left|b(t) - a_j(t)\right| \to 0$ exponentially. The theorem is then proved. ∎

With the following result we address the case where the invariant subspaces defined by the symmetries are not strictly contained in each other but intersect.

Theorem 7. Assume that $\mathcal{M}_\cap = \cap\mathcal{M}_i \neq \{0\}$. Then, all solutions of Eq. (1) exhibit the symmetry defined by $\mathcal{M}_\cap$ if one of the two conditions holds: (i) f is contracting toward each subspace $\mathcal{M}_i$ or (ii) f is contracting.

Proof. Let x_i, $i = 1,\dots,s$, be solutions of Eq. (1), such that $x_i(0) \in \mathcal{M}_i$, and $a(t)$ be a solution of the system such that $a(0) \notin \mathcal{M}_i$. Now, if f is contracting toward each $\mathcal{M}_i$, we have, by definition, that there exists $K_i > 0$, $\lambda_i > 0$, $i = 1,\dots,s$, such that $|a(t) - x_i| \leqslant K_i e^{-\lambda t}$. This, in turn, implies that there exists some $K > 0$, $\lambda > 0$ such that $\left|x_i - x_j\right| \leqslant K e^{-\lambda_i t}$, $\quad \forall i \neq j$. Now, since $\mathcal{M}_i$ are flow invariant, we have that $x_i(t) \in \mathcal{M}_i$, for all $t \geqslant 0$. Thus, $x_i(t) \to \mathcal{M}_\cap$, as $t \to +\infty$, implying that also $a \to \mathcal{M}_\cap$, as $t \to +\infty$. By using similar arguments, it is possible to prove the result under the stronger hypothesis of f being contracting. ∎

We remark here that in the context of networked systems, Theorems 6 and 7 can be stated by using balance equivalence relations (see Ref. [11]).

1. Synchronizing networks with chain topologies

As a first application of our results we revisit the problem of finding sufficient conditions for the synchronization of networks having chain topologies. Specifically, we show that Theorem 6 allows to study network synchronization iteratively reducing the dimensionality of the problem. For the sake of clarity we now consider a simple network of four nodes. While developing the example, we will also introduce introduce an important γ symmetry (i.e., permutations).

Consider the diffusively coupled network represented in Fig. 1, whose dynamics are described by

$$\begin{aligned} \dot{x}_1 &= f_1(X) = g(x_1) + h(x_2) - h(x_1) \\ \dot{x}_2 &= f_2(X) = g(x_2) + h(x_1) + h(x_3) - 2h(x_2) \\ \dot{x}_3 &= f_3(X) = g(x_4) + h(x_2) + h(x_4) - 2h(x_3) \\ \dot{x}_4 &= f_4(X) = g(x_4) + h(x_3) - h(x_4), \end{aligned} \tag{3}$$

where $x_i \in \mathbb{R}^n$, $X = [x_1^T, x_2^T, x_3^T, x_4^T]^T$, all the nodes have the same intrinsic dynamics, g and are coupled by means of the output function, h. The set of ordinary differential equations (ODEs) (3) are studied in Ref. [10] as they represent linear chains with bidirectional diffusive coupling and Neumann boundary conditions. Moreover, in Ref. [22], an explanation of the patterns of symmetry for these networks is given. In this section, we show that a contracting property of vector fields selects one of the possible synchrony patterns, making it globally exponentially stable.

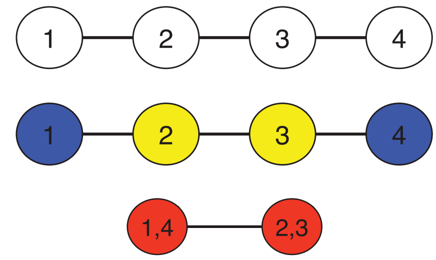

FIG. 1. (Color online) Top panel: the chain topology network of four nodes. Middle panel: polysynchronous subspace identified by $\mathcal{M}_2$. Bottom panel: equivalent network and synchronous subspace identified by $\mathcal{M}_1$. The graphs presented in this figure are linear chains with bidirectional diffusive coupling and Neumann boundary conditions (see Ref. [10]).

Now, consider the following action:

$$\gamma_2 : (x_1, x_2, x_3, x_4) \to (x_4, x_3, x_2, x_1). \tag{4}$$

That is, γ_2 permutes x_1 with x_4 and x_2 with x_3. Let $F(X) = [f_1(X)^T, f_2(X)^T, f_3(X)^T, f_4(X)^T]^T$: It is straightforward to check that $\gamma_2 F(X) = F(\gamma_2 X)$. That is, F is Γ_2 equivariant. This, in turn, implies the existence of the flow-invariant subspace

$$\mathcal{M}_2 = \{X \in \mathbb{R}^{4n} : (x_1, x_2, x_3, x_4) = (x_4, x_3, x_2, x_1)\}.$$

Notice that such a subspace corresponds to the polysynchronous subspace [22], where node 1 is synchronized to node 4 and node 2 is synchronized to node 3 (synchronous nodes are also pointed out in Fig. 1). Let $J_2(X)$ be the Jacobian of the network, and

$$V_2 = \frac{1}{\sqrt{2}}\begin{bmatrix} -1 & 0 & 0 & 1 \\ 0 & -1 & 1 & 0 \end{bmatrix}$$

be the matrix spanning the null of $\mathcal{M}_2$ (notice that the rows of $\mathcal{M}_2$ are orthonormal). All the trajectories of the network globally exponentially converge toward $\mathcal{M}_2$ if the matrix $V_2 J_2(X) V_2^T$ is contracting (see Theorem 4). It is straightforward to check that such a matrix is contracting if the function $g(\cdot) - h(\cdot)$ is contracting. Let $x_{1,4}, x_{2,3} \in \mathcal{M}_2$, with $x_{1,4} = x_1 = x_4$ and $x_{2,3} = x_2 = x_3$; the dynamics of Eq. (3) reduced on $\mathcal{M}_2$ is given by

$$\begin{aligned} \dot{x}_{1,4} &= g(x_{1,4}) + h(x_{2,3}) - h(x_{1,4}) \\ \dot{x}_{2,3} &= g(x_{2,3}) + h(x_{1,4}) - h(x_{2,3}), \end{aligned} \tag{5}$$

which corresponds to an equivalent two-node network (see Fig. 1). It is straightforward to check that the above reduced dynamics is Γ_1 equivariant with respect to the action

$$\gamma_1 : (x_{1,4}, x_{2,3}) \to (x_{2,3}, x_{1,4}).$$

Thus, the subspace

$$M_1 = \{X \in \mathbb{R}^{4n} : (x_{1,4}, x_{2,3}) = (x_{2,3}, x_{1,4})\}$$

is a flow-invariant subspace. Furthermore, the trajectories of Eq. (5) globally exponentially converge toward $\mathcal{M}_1$ if $V_1 J_1(X) V_1^T$ is contracting, where $V_1 = \frac{1}{\sqrt{2}}[-1, 1]$ and $J_1(X)$

is the Jacobian of Eq. (5). Now, $V_1 J_1 V_1^T = \frac{1}{2}(\frac{\partial g}{\partial x_{1,4}} - 2\frac{\partial h}{\partial x_{1,4}} + \frac{\partial g}{\partial x_{2,3}} - 2\frac{\partial h}{\partial x_{2,3}})$, which is contracting if $g(\cdot) - h(\cdot)$ is contracting.

Thus, using Theorem 6, we can finally conclude that the network synchronizes if the function

$$g(\cdot) - h(\cdot) \tag{6}$$

is a contracting function. Notice that this also implies that the synchronization subspace is unique.

We remark the following here:

(i) the dimensionality-reduction methodology presented above can be also extended to the more generic case of chain topologies of length 2^r, for any integer, r.

(ii) the same methodology can be used to prove synchronization of networks having hypercube topologies, as they can be seen as chains of chains. Hence, the above approach can be used to find condition for the synchronization of lattices. Such a topology typically arises from, for example, the discretization of partial differential equations. In this view, our results provide a sufficient condition for the spatially uniform behavior in reaction diffusion partial differential equations (PDEs), similarly to Ref. [23].

(iii) the synchronization condition in Eq. (6) is less stringent than that obtained by proving contraction of Eq. (3) toward the synchronization subspace $\mathcal{M} = \{X \in \mathbb{R}^{4n} : x_1 = x_2 = x_3 = x_4\}$.

B. Generalizations using virtual systems

The results presented in the previous sections link the symmetries of a dynamical system and contraction. Specifically, they show that if a system presents a set of $s > 1$ symmetries, then the final behavior is determined by the contraction properties of the vector field.

In this section, we extend the previous results and show that in order for the solutions of Eq. (1) to exhibit a specific symmetry, equivariance and contraction of f are not necessarily needed. Indeed, such a condition can be replaced by a weaker condition: namely, an equivariance condition on the vector field of some auxiliary (or virtual) system, similar in spirit to Theorem 2.

Theorem 8. Consider the system

$$\dot{y} = v(y,x,t) \tag{7}$$

where $x(t)$ are the solutions of Eq. (1) and $v(x,y,t)$ is some smooth function such that

$$v(x,x,t) = f(x,t).$$

The following statements hold:

(i) if $v(y,x,t)$ is Γ equivariant and contracting toward $\mathcal{M}_\gamma$, then any solution of Eq. (1) converges toward a γ-symmetric solution.

(ii) if $v(y,x,t)$ is h equivariant and contracting, then any solution of Eq. (1) converges toward an h-symmetric solution.

System (7) is termed a virtual system.

Proof. Indeed, by assumption, all the solutions $y(t)$ of the virtual system globally exponentially converge toward some h (γ) symmetric solution, say $x(t)$. Now, notice that any solution of Eq. (1), say $a(t)$, is a particular solution of Eq. (7), since $v(x,x,t) = f(x,t)$. This implies that

$$|a(t) - x(t)| \to 0$$

as $t \to +\infty$. The result is then proved. ■

A simple example illustrating the key features of Theorem 8 is as follows. Consider the dynamical system

$$\dot{x} = -(e^x + 1)x,$$

which can be easily shown to be not contracting and to have no symmetries. We will show, by means of Theorem 8, that there exists a symmetric virtual system proving that the final behavior of the original system is symmetric. Indeed, consider the virtual system

$$\dot{y} = -(e^x + 1)y.$$

Clearly, such a system has the symmetry $y \to -y$. Therefore, Theorem 8 implies that all the solutions of the original system converge toward the symmetric solution, explaining the fact that final behavior of the original system is symmetric.

Note the following:

(i) Any solution of the virtual system having symmetric initial conditions [i.e., $y(0) = \gamma y(0)$] preserves the symmetry for any $t > 0$. In particular, if a solution of the real system has initial conditions verifying the symmetry of the virtual system [i.e., $x_0 = \gamma x_0$] then it preserves this symmetry [i.e., $x(t) = \gamma x(t)$] for any $t \geqslant 0$. This is a generalization of the basic result presented in Sec. II B.

(ii) Theorem 8 can be straightforwardly extended to the case where the virtual system presents a set of $s > 1$ spatial symmetries. Analogous results to Theorems 6 and 7 can be easily proven.

1. *A discussion on symmetries of virtual systems*

Let us briefly discuss some of the main features of our results involving the use of virtual systems.

We showed that a given dynamical system of interest can exhibit some symmetric final behavior even if the corresponding vector field is not equivariant and/or contracting. Indeed, a sufficient condition for a system to exhibit a symmetric final behavior is the symmetry of the vector field of some appropriately constructed virtual system. Of course, an interesting general question is that of identifying a virtual system explaining the final behavior of a real system, an aspect is reminiscent of the process of identifying a Lyapunov function in stability analysis.

The idea of relating behaviors of real systems using a symmetric virtual system, possibly of different dimension, presents analogies with the concept of supersymmetry in particle physics (see, e.g., Refs. [24,25] and references therein). The motivation beyond the concept of supersymmetry is that nonsymmetric transformations of an object (the real system in our framework) in a finite dimensional space, may be explained by a symmetric transformation of another, possibly higher-dimensional object (the virtual system in our framework).

Finally, we remark here that all the results presented above can be straightforwardly extended to address the problem of designing control strategies guaranteeing convergence of a system of interest onto some desired trajectory. Intuitively, the idea is that the control input has to: (i) generate some desired symmetry for the vector field (and hence some desired invariant subspace defining the system's final behavior) and (ii) drive all the trajectories toward the invariant subspace imposing contraction.

IV. SYSTEM WITH INPUTS

In the above sections, we presented some results that can be used to analyze the final behavior of a system of interest. The main idea beyond such results is the use of contraction to study convergence of trajectories toward some invariant subspace. In turn, such a subspace is defined by some structural property of the vector field, namely a symmetry.

We now generalize this result further, and show that it is possible to determine a direct relation between the trajectories of a system when forced by different classes of inputs. The results presented in this section are also based on the concept of virtual system. Indeed, while the forced systems of interest considered here are not equivariant and/or contracting, we will show that it is possible to construct a symmetric and contracting virtual system that allows us to relate the final behavior of the two systems.

Consider a system described by

$$\dot{x} = f(x,u(t),t). \tag{8}$$

The following result holds:

Theorem 9. Assume that Eq. (8) is contracting with respect to x, uniformly in $u(t)$, and that there exist some linear transformations γ_i, ρ_i, $i \geqslant 1$, such that: $\gamma_i f(x,u(t),t) = f(\gamma_i x,\rho_i u(t),t)$. Let $x_i(t)$ be a solution of Eq. (8) when forced by $u(t) = u_i(t)$ [i.e. $\dot{x}_i = f(x_i,u_i(t),t)$ $x_i(t=0) = x_{0,i}$]. Then, for any $u_i(t)$, $u_j(t)$ such that $\rho_i u_i(t) = \rho_j u_j(t)$

$$|\gamma_i x_i - \gamma_j x_j| \to 0$$

as $t \to +\infty$. Moreover, let x_i^k and x_j^k the kth component of x_i and x_j, respectively and γ_i^k, (γ_j^k) be the kth component of γ_i (γ_j). If $\gamma_i^k x_{0,i}^k = \gamma_j^k x_{0,j}^k$ then $\gamma_i^k x_i^k(t) = \gamma_j^k x_j^k(t)$, for any $t \geqslant 0$.

The second statement of the above theorem implies that if the system when forced by two different inputs starts with certain symmetries, then the symmetries are preserved.

Proof. Indeed, let $u_v = \rho_i u_i = \rho_j u_j$ and consider the following virtual system:

$$\dot{y} = f(y,u_v,t). \tag{9}$$

Notice that, for any i, j, $\gamma_i x_i$, and $\gamma_j x_j$ are particular solutions of such a system. Indeed:

$$\gamma_i \dot{x}_i = \gamma_i f(x_i,u_i,t) = f(\gamma_i x_i,\rho_i u_i,t) = f(\gamma_i x_i,u_v,t)$$
$$\gamma_j \dot{x}_j = \gamma_j f(x_j,u_j,t) = f(\gamma_j x_j,\rho_j u_j,t) = f(\gamma_j x_j,u_v,t).$$

Now, since $f(x,u_v,t)$ is contracting by hypotheses, we have, for any i, j, there exists some C such that

$$|\gamma_i x_i - \gamma_j x_j| \leqslant C|\gamma_i x_{0,i} - \gamma_j x_{0,j}|e^{-\lambda t}, \quad \lambda > 0.$$

This proves the first part of the result. To conclude the proof it suffices to notice that exponential convergence of $|\gamma_i x_i - \gamma_j x_j|$ to 0 implies that all of its components exponentially converge to 0. In particular, this implies that there exists some C_k, λ_k such that

$$\left|\gamma_i^k x_i^k - \gamma_j^k x_j^k\right| \leqslant C_k\left|\gamma_i^k x_{0,i}^k - \gamma_j^k x_{0,j}^k\right|e^{-\lambda t_k}, \quad \lambda_k > 0.$$

Since $|\gamma_i^k x_{0,i}^k - \gamma_j^k x_{0,j}^k| = 0$ by hypotheses, we have that $|\gamma_i^k x_i^k(t) - \gamma_j^k x_j^k(t)|$ $\forall t \geqslant 0$. ∎

Theorem 9 can be extended by replacing the linear operators γ_i, ρ_i by more general nonlinear transformations acting on the system

$$\dot{x} = f(x,u(x,t),t). \tag{10}$$

The transformations considered are smooth nonlinear functions of the state and of time, $\gamma = \gamma(x,t)$, $\rho = \rho(u(x,t),x,t)$. Following the same arguments as in Theorem 9, it is then straightforward to show:

Theorem 10. Assume that Eq. (10) is contracting uniformly in $u(x,t)$ and that there exist some $\gamma_i(x,t)$, $\rho_i(u(x,t),x,t)$, $i \geqslant 1$, such that

$$\frac{\partial \gamma_i}{\partial x} f(x,u(x,t),t) = f(\gamma_i(x),\rho_i(u(x,t),x,t),t)$$

Let $x_i(t)$ be solutions of Eq. (10) when forced by $u(t) = u_i(x_i,t)$ [i.e., $\dot{x}_i = f(x_i,u_i(x_i,t),t)$, $x_i(t=0) = x_{0,i}$]. Then, for any $u_i(x_i,t)$, $u_j(x_j,t)$ such that $\rho_i(u(x_i,t),x_i,t) = \rho_j(u_j(x_j,t),x_j,t)$

$$|\gamma_i(x_i) - \gamma_j(x_j)| \to 0$$

as $t \to +\infty$. Moreover, let x_i^k and x_j^k the kth component of x_i and x_j, respectively and γ_i^k, (γ_j^k) be the kth component of γ_i (γ_j). If

$$\gamma_i^k\left(x_{0,i}^k\right) = \gamma_j^k\left(x_{0,j}^k\right)$$

then $\gamma_i^k(x_i(t)^k) = \gamma_j^k(x_j(t)^k)$, for any $t \geqslant 0$.

Proof. The proof follows exactly the same steps as those used to prove Theorem 9, with u_v in virtual system Eq. (9) now being chosen as $u_v = \rho_i(u(x_i,t),x_i,t) = \rho_j(u_j(x_j,t),x_j,t)$. ∎

We close this section by pointing out some features of the above two theorems.

(i) The proofs of both Theorems 9 and 10 are based on the proof of contraction of some appropriately constructed virtual system of the form of Eq. (9). We now show that, if some hypotheses are made on γ_i, then the contraction condition can be weakened. Specifically, assume that all the intersection of the subspaces defined by γ_i, $\mathcal{M}_i$, is nonempty. Then, it is straightforward to check that $\left|\gamma_i x_i - \gamma_j x_j\right| \to 0$ if f is contracting toward each $\mathcal{M}_i$, or contracting toward $\mathcal{M}_\cap$. Notice that, since our results make use of symmetries of virtual systems, they extend those in Ref. [9].

(ii) Analogously, Theorems 9 and 10 can also be extended to study the case where the input u_i selects one specific symmetry γ_i. Indeed, let $u_v = \rho_i u_i$. In this case, it can be shown that symmetry γ_i is shown by the solutions of Eq. (8) if $f(x,u_v,t)$ is contracting toward $\mathcal{M}_i$.

(iii) A particularly interesting case for Theorem 9 is when some of the components of $x_{0,i}$ and $x_{0,j}$ are the same and the actions γ_i and γ_j leave such components unchanged. That is, in view of the notations above $\gamma_i^k = id = \gamma_j^k$ and $x_{0,i}^k = x_{0,j}^k$. Indeed, in this case Theorem 9 implies that $x_i^k(t) = x_j^k(t)$, $\forall t \geqslant 0$. That is, the kth components of the trajectories of Eq. (8) have identical temporal evolutions even if forced by different inputs. A similar result holds for Theorem 10. This consequence of the above two results is used in Sec. V.

V. EXAMPLE: INVARIANCE UNDER INPUT SCALING

In a series of recent papers, input-output properties of some cellular signaling biochemical systems have been analyzed [26–29]. Such studies point out that many sensory systems show the property of having their output invariant under input scaling, which can be formally defined as follows.

Definition 5. Let $x_i(t)$, $x_j(t)$ be solutions of Eq. (8) with initial conditions $x_0 = x_i(0) = x_j(0)$, when $u(t) = \chi_i(t)$ and $u(t) = \chi_j(t)$, respectively. System Eq. (8) is invariant under input scaling if $x_i(t) = x_j(t)$ for any $\chi_i(t)$, $\chi_j(t)$ such that $\chi_j(t) = F(t)\chi_i(t)$, with $F(t) > 0$.

Invariance under input scaling with constant $F(t) = F$ has been recently studied in transcription networks by Alon and his coauthors [26,27,29]. In such papers, the authors focus on the study of transcriptional networks subject to step inputs. In this case, the invariance under input scaling is called fold-change detection behavior (FCD), as the output of the system depends only on fold changes in input and not on its absolute level. For example, if the input to the system is a step function from 1 to 2, then its output is the same as if the step was increased from 2 to 4.

This section uses this paper's results to analyze the associated mathematical models, arising from protein signal-transduction systems and bacterial chemotaxis, and in particular it revisits the recent work [27] from this point of view. It also shows how these results could, for instance, suggest a mechanism for stable quorum sensing in bacterial chemotaxis, thus combining symmetries in cell interactions (quorum sensing) with invariance to input scaling (fold-change detection).

A. Gene regulation

This first example considers a pattern (network motif) arising in gene regulation networks, the Type 1 Incoherent Feed-Forward Loop (I1-FFL) [30,31]. The I1-FFL is one of the most common network motifs in gene regulation networks (see also Sec. VII). As shown in Fig. 2, it consists of an activator, X, which controls a target gene, Z, and activates a repressor of the same gene, Y (which can be thought of as the output of the system). It has been recently shown that such a network motif can generate a temporal pulse of Z response, accelerate the response time of Z, and act as a band-pass amplitude filter (see, e.g., [32,33]).

In Ref. [26] it has also been shown by using a dimensionless analysis that for a certain range of biochemical parameters, the I1-FFL can exhibit invariance under step-input scaling (i.e., FCD).

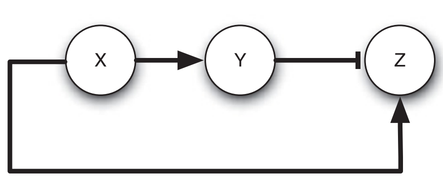

FIG. 2. A schematic representation of the I1-FFL.

1. A basic model

In Ref. [26], it was shown that a minimal circuit that achieves FCD is the I1-FFL, with the activator in linear regime and the repressor saturating the promoter of the target gene, Z. The model in Ref. [26] is of the form

$$\dot{Y} = -\alpha_1 Y + \chi(t)$$
$$\dot{Z} = \beta_2 \frac{\chi(t)}{Y} - \alpha_2 Z \qquad (11)$$

where α_1, α_2, β_2 are biochemical (positive) parameters and $\chi(t)$ is the input to the system (which can be approximated by the concentration of X). It was also shown that the dimensionless model

$$\frac{dy}{d\tau} = F - y$$
$$r\frac{dz}{d\tau} = \frac{F}{y} - z$$

with

$$y = \frac{Y\alpha_1}{\beta_1 \chi_{\min}} \quad Z = \frac{Z}{\beta_2\alpha_1/\beta_1\alpha_2}$$
$$F = \frac{\chi(t)}{\chi_{\min}} \qquad \tau = \alpha_1 t$$

exhibits invariance under input scaling. In Sec. VII, we will also analyze other important network motifs under a slightly different viewpoint (i.e., by considering each of the species composing the motif as nodes of an interconnected systems).

In this section, we show invariance under input scaling for system Eq. (11) for any input, $\chi_i(t)$, $\chi_j(t)$, such that $\frac{\chi_i(t)}{\chi_{\min,i}} = \frac{\chi_j(t)}{\chi_{\min,j}} = F(t)$. In the above expressions $\chi_{\min,i}$ and $\chi_{\min,j}$ denote the basal level of the inputs $\chi_i(t)$ and $\chi_j(t)$ respectively. Such levels are assumed to be nonzero. Notice that the above class of inputs is wider that the one used in Definition 5.

Theorem 9 is now used to prove invariance under input scaling for Eq. (11). That is, we show that invariance under input scaling is a consequence of the existence of a symmetric and contracting virtual system in the spirit of Theorem 9.

In what follows, we will denote with $x_i = (Y_i, Z_i)^T$ and $x_j = (Y_j, Z_j)^T$ the solutions of Eq. (11), when $\chi(t) = \chi_i(t)$ and $\chi(t) = \chi_j(t)$, respectively. We assume that $Z_i(0) = Z_j(0)$. In terms of the notation introduced in Theorem 9, we have $u(t) = \chi(t)$ and

$$f(x, u(t)) = \begin{pmatrix} -\alpha_1 Y + \chi(t) \\ \beta_2 \frac{\chi(t)}{Y} - \alpha_2 Z \end{pmatrix}.$$

Now, define the following actions:

$$\gamma_i = \begin{pmatrix} Y \\ Z \end{pmatrix} \rightarrow \begin{pmatrix} \frac{Y}{\chi_{\min,i}} \\ Z \end{pmatrix}, \quad \rho_i : \chi(t) \rightarrow \frac{\chi(t)}{\chi_{\min,i}} = F(t). \tag{12}$$

It is straightforward to check that $f(x,u(t))$ is contracting uniformly in $u(t)$ and $\gamma_i f(x_i,\chi_i(t)) = f(\gamma_i x_i, \rho_i \chi_i(t))$. Now, Theorem 9 implies that for any input $\chi_i(t)$, $\chi_j(t)$ such that $\rho_i \chi_i(t) = \rho_j \chi_j(t)$, $\gamma_i x_i$ and $\gamma_j x_j$ globally exponentially converge toward each other. That is

$$|\gamma_i x_i - \gamma_j x_j| = \left| \begin{pmatrix} \frac{Y_i}{\chi_{\min,i}} - \frac{Y_j}{\chi_{\min,j}} \\ Z_i - Z_j \end{pmatrix} \right| \rightarrow 0 \tag{13}$$

for any χ_i, χ_j such that

$$\frac{\chi_i(t)}{\chi_{\min,i}} = \frac{\chi_j(t)}{\chi_{\min,j}} = F(t). \tag{14}$$

Now, Eq. (13) implies that $|Z_i - Z_j| \rightarrow 0$ exponentially. Since the initial conditions of Z_i and Z_j are the same we have that $Z_i(t) = Z_j(t)$ for any $t \geqslant 0$. That is, the system exhibits invariance under input scaling.

B. A model from chemotaxis

In bacterial chemotaxis, bacteria walk through a chemo-attractant field, say $u(t,r)$ (r denotes two dimensional space vector). Along their walk, bacteria sense the concentration of u at their position and compute the tumbling rate (rate of changes of the direction) so as to move toward the direction where the gradient increases (see, e.g., Ref. [34]). Typically, the input field is provided by means of a source of attractant that diffuses in the medium with bacteria accumulating in the neighborhood of the source. In this case, the information on the position of the source is encoded only in the shape of the field and not in its strength. Therefore, it is reasonable for bacteria to evolve a search pattern that is dependent only on the shape of the field and not on its strength (i.e., a search pattern that is invariant under input scaling [27]). Specifically, consider the following model [27] adapted from the chemotaxis model of Ref. [35]:

$$\begin{aligned} \dot{x} &= x f(y) \\ \epsilon \dot{y} &= \phi\left(\frac{u}{x}\right) - y \end{aligned} \tag{15}$$

where $u > 0$ is an increasing step input to the system, representing the ligand concentration, and $y > 0$, the output of the system, represents the average kinase activity. The quantity $x > 0$ is an internal variable. We assume the function ϕ to be a decreasing function in x with bounded partial derivative $\partial\phi/\partial x$ and an increasing function of u/x, with derivative $\phi' = \partial\phi/\partial(u/x) \leqslant b$, $b > 0$. Note that the above model becomes the one used in Ref. [27], when $\phi(u/x) = u/x$. Such a model is obtained assuming x is sufficiently large, with the term u/x actually a simplification of a term of the form $u/(x+\eta)$, with $0 < \eta \ll x$. The positive constant ϵ is typically small, so as to represent a separation of time scales.

Assume as in Ref. [35] that $f(1) = 0$ and that $f(y)$ is strictly increasing with y. Obviously, Eq. (15) verifies the symmetry conditions of Theorem 9 with

$$\gamma_i : (x_i, y_i) \rightarrow \left(\frac{x_i}{\bar{u}_i}, y_i\right), \quad \rho_i : u_i \rightarrow \frac{u_i}{\bar{u}_i} \tag{16}$$

where $\bar{u}_i$ denotes the initial (lower) value, at time $t = 0$, of the step function. As in the preceding section we assume that $y_i(0) = y_j(0)$. Now, by means of Theorem 9, we can conclude that, if the system is contracting, $y_i(t) = y_j(t)$, $\forall t \geqslant 0$, for any input such that $\frac{u_i}{\bar{u}_i} = \frac{u_j}{\bar{u}_j} = F$.

Let us derive a condition for Eq. (15) to be contracting, which will give conditions on the dynamics and inputs of Eq. (15) ensuring invariance under input scaling. Model Eq. (15) can be recast as

$$\ddot{y} + \frac{1}{\epsilon}\dot{y} - \frac{1}{\epsilon}\frac{\partial\phi}{\partial x} x f(y) = 0. \tag{17}$$

As in Refs. [27,35], choose $f(y) = y - 1$ for simplicity, so that Eq. (17) becomes

$$\ddot{y} + \frac{1}{\epsilon}\dot{y} - \frac{1}{\epsilon}\frac{\partial\phi}{\partial x} x(y-1) = 0. \tag{18}$$

The above dynamics is similar to a mechanical mass-spring-damper system with a time-varying spring, $\ddot{r} + 2\eta\omega\dot{r} + \omega^2 r = 0$ with $2\eta\omega = \frac{1}{\epsilon}$ and $\omega^2 = -\frac{1}{\epsilon}\frac{\partial\phi}{\partial x}x$. Now, as shown in Ref. [36] such a dynamics is contracting if $\eta > \frac{1}{\sqrt{2}}$. Thus, it immediately follows that Eq. (18) is contracting if

$$\frac{\partial\phi}{\partial x} x > -\frac{1}{2\epsilon}. \tag{19}$$

Hence, contraction is attained if $\phi'(-\frac{u}{x^2})x > -\frac{1}{2\epsilon}$ That is, a sufficient condition for Eq. (18) to be contracting is

$$x > 2\epsilon u b. \tag{20}$$

Notice that, in the case where $\phi(u/x) = u/x$, Eq. (20) simply becomes

$$x > 2\epsilon u. \tag{21}$$

The above inequality implies that, in this case, the system is contracting (and hence exhibits invariance under input scaling) if the level of x is sufficiently high (which is true by hypotheses) and its dynamics is sufficiently slow (ϵ small) with respect to the dynamics of y. Also, given $\varepsilon < \frac{1}{2}$ and a constant u, if contraction condition Eq. (21) is verified at $t = 0$ with initial conditions embedded in a ball contained in the contraction region in Eq. (21), it remains verified for any $t \geqslant 0$.

Finally, note that the results of this section, and indeed of the original [26,27], are closely related to the idea, first introduced in Ref. [8] and further studied in Ref. [9], of detecting a symmetry (here, in the environment) by using a dynamic system having the same symmetry.

VI. ANALYSIS AND CONTROL OF INTERCONNECTED SYSTEMS

The results presented in the preceding section indicate that there exists a direct link between symmetries of a (virtual) vector field and of its solutions, if the system is contracting (or it is made contracting by some control input).

The aim of this section is that of using the above results to analyze and control the (poly)synchronous behavior of

$N > 1$ (possibly heterogeneous) interconnected systems (also termed as networks in what follows). Such a behavior has been recently reported in ecological systems, networks characterized by strong community structure and in bipartite networks consisting of two groups (see, e.g., [37–39]). For interconnected systems, symmetries are essentially defined by the nodes' dynamics, the topology of the network, and by the particular choice of the coupling functions. The definitions and and framework introduced in what follows were introduced by Golubitsky and Stewart in a number of works (see Refs. [10–12]).

A. Definitions

In our framework the phase space of the ith node (or cell, or neuron) is denoted with P_i, while its state at time t is denoted with $x_i(t)$. Notice that P_i could in general be a manifold. Each node has an intrinsic dynamics, which is affected by the state of some other nodes (i.e., the neighbors of i) by means of some coupling function. Those interactions will be represented by means of directed graphs. In such a graph the nodes having the same internal dynamics will be represented with the same symbol. Analogously, heterogeneous coupling functions can be taken into account: Identical functions will be denoted by the same symbol. This is formalized with the following.

Definition 6. An interconnected system consists of: (i) a set of nodes $\mathcal{N} = \{1, \ldots, N\}$; (ii) an equivalence relation, $\sim_{\mathcal{N}}$ on $\mathcal{N}$; (iii) a finite set, $\mathcal{E}$, of edges (arrows); (iv) an equivalence relation, $\sim_{\mathcal{E}}$ on $\mathcal{E}$; (v) the maps $\mathcal{H} : \mathcal{E} \to \mathcal{N}$ and $\mathcal{T} : \mathcal{E} \to \mathcal{N}$ such that: for $e \in \mathcal{E}$, we have $\mathcal{H}(e)$ is the head of the arrow and $\mathcal{T}(e)$ the tail of the arrow; (vi) equivalent arrows have equivalent tails and heads. That is, if $e_1, e_2 \in \mathcal{E}$ and $e_1 \sim_{\mathcal{E}} e_2$, then $\mathcal{H}(e_1) \sim_{\mathcal{N}} \mathcal{H}(e_2)$ and $\mathcal{T}(e_1) \sim_{\mathcal{N}} \mathcal{T}(e_2)$.

We say that an edge $e \in \mathcal{E}$ is an input edge to a node, say i, if $\mathcal{H}(e) = i$. The set of input edges to node i is termed as input set and denoted by $\mathcal{I}(i)$. We also say that two nodes, say c and d, are input equivalent if there exists an arrow type preserving bijection, $\beta : \mathcal{I}(c) \to \mathcal{I}(d)$.

Finally, our setup is completed by defining the dynamics of an interconnected system as follows.

Definition 7. The dynamical system

$$\dot{X} = F(X,t) \tag{22}$$

defines an interconnected system if its phase space is defined as $P = P_1 \times \cdots P_N \times \mathbb{R}^+$ where P_i denotes the phase space of the ith network node. Furthermore, let $\pi_i : P \to P_i$ be projections of Eq. (22), then it must hold that $\pi_i(X(t)) = x_i(t)$.

In Ref. [10], all the possible invariant polydiagonals, defining a specific synchronization pattern, for networks of ODEs are classified by using the notion of balanced colorings. In the next section, we show that a contracting property on network dynamics selects a specific pattern of symmetry, determining, among all the possible final behaviors, the one that is shown by the network.

B. Analysis and control

Let: $P_1 \subseteq \mathbb{R}^{n_1}$, $P_2 \subseteq \mathbb{R}^{n_2}$, ..., $P_N \subseteq \mathbb{R}^{n_N}$ be convex subsets, $P = P_1 \times \cdots \times P_N$, $X = [x_1^T, \ldots, x_N^T]^T$, $x_i \in P_i$, $\phi_i : P \times \mathbb{R}^+ \to P_i$ be smooth functions. In what follows, we consider systems of the form

$$\dot{x}_i = \phi_i(X,t) = f_i(x_i,t) + \tilde{h}_i(X,t) \tag{23}$$

with $i = 1, \ldots, N$. Notice that Eq. (23) represents an interconnected system (Definition 7). Specifically, in Eq. (23) the function $f_i : P_i \times \mathbb{R}^+ \to P_i$ is the intrinsic dynamics of the ith node, while the function $\tilde{h}_i : P \times \mathbb{R}^+ \to P_i$ describes the interaction of the ith node with the other nodes composing the interconnected system.

Notice that the above formalization allows us to consider within a unique framework directed and undirected networks, self loops, and multiple interactions. We will also consider networks with (smoothly) changing topology.

The main idea of this section for the study of the collective polysynchronous behavior emerging in network Eq. (23) can be stated as follows: Study symmetries of Eq. (23) to determine the possible patterns of synchrony and determine among the possible patterns, the one exhibited by Eq. (23) using contraction properties.

Consider a partition of the N nodes of a network into k groups, $\mathcal{G}_1, \ldots, \mathcal{G}_k$, characterized by the same intrinsic dynamics. We define the following invariant subspaces associated to each group of nodes:

$$\mathcal{M}_{p,s} = \{x_i = x_j, \ \forall i,j \in \mathcal{G}_s\}, \quad s = 1, \ldots, k$$

Notice that all the nodes of the ith group are synchronous if and only if network dynamics evolve onto the associated subspace $\mathcal{M}_{p,i}$. The polysynchronous subspace, say $\mathcal{M}_p$, is then defined as the intersection of all $\mathcal{M}_{p,s}$ (i.e., $\mathcal{M}_p = \cap_s \mathcal{M}_{p,s}$) or equivalently

$$\mathcal{M}_p = \{x_i = x_j, \ \forall i,j \in \mathcal{G}_m, 1 \leqslant m \leqslant k\}.$$

We say that a pattern of synchrony is possible for the network of interest if its corresponding polysynchronous subspace is flow invariant. In this view, a useful result is the following.

Theorem 11. The set $\mathcal{M}_p$ is invariant for network Eq. (22) if the nodes belonging to group $\mathcal{G}_p$ have the same uncoupled dynamics and are input equivalent.

Specifically, Theorem 11 is indeed a consequence of the fact that input equivalence is always a balanced equivalence relation (see Refs. [1,11]). In terms of network synchronization, intuitively such a result implies that a specific pattern of synchrony is possible if the aspiring synchronous nodes have synchronous input sets.

The following result is a straightforward consequence of the results of the preceding section on spatial symmetries.

Corollary 1. Assume that for network Eq. (23) the sets $\mathcal{M}_{p,s}$ exist. Then, the synchrony pattern exhibited by the network is given by: (i) $\mathcal{M}_p$, if the network is contracting, or contracting toward each $\mathcal{M}_{p,s}$; (ii) $\mathcal{M}_{p,s}$, if the network is contracting toward $\mathcal{M}_{p,s}$.

One of the applications where the above results can be used is that of designing networks performing specific tasks. For example, in Ref. [8] it was shown that a network with a specific symmetry can be used to detect symmetries of images, for example. Our results can be used to extend this framework. Indeed, each network node in Eq. (23) may be used to process some exogenous input, $U(t) = [u_1, \ldots, u_N]$, i.e.,

$$\dot{x}_i = \phi_i(X,t) = f_i(x_i,t) + \tilde{h}_i(X,t) + u_i(t).$$

Now, while u_i denotes the information that has to be processed by node i, the couplings $\tilde{h}_i$ may be seen as an input (typically, sparse) acting on the couplings between nodes, so as to activate

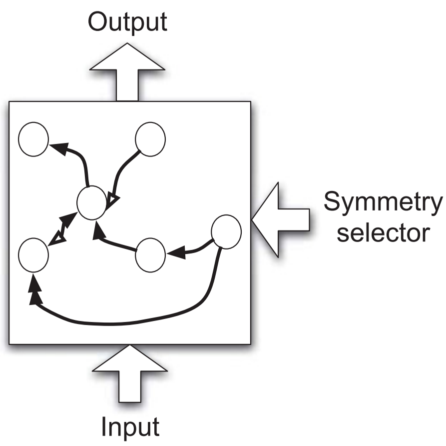

FIG. 3. A schematic representation of a network used to process information. In our framework, the network is subject to two kinds of inputs: $\bar{U}(t)$ and $\tilde{U}(X)$. In particular, $\bar{U}(t)$ can be seen as the information processed by the network: Such input can activate some intrinsic symmetries of the network. On the other hand, $\tilde{U}(X)$ is a typically sparse input that acts on the coupling functions so as to force the activation of some desired symmetry of the interconnected system.

a desired, arbitrary symmetry. The output of the network is then some desired synchronous pattern that arises from the intersection of the symmetries activated by $\bar{U}(t)$ and those activated by $\tilde{U}(X)$. Figure 3 schematically illustrates this principle.

For instance, assume that the system consists of a large number of synchronized oscillators. Then we know [15] that with an adequate choice of coupling gains adding a single inhibitory connection between any two nodes will make the entire system contracting and therefore will stop the oscillations and adding a leader oscillator (i.e., an oscillator with only feed-forward connections to the rest of the network, its neighbors for instance) will make the entire system get in phase with the leader. Thus very sparse feedback inputs can completely change the symmetries of the system, and therefore its symmetry detection specifications.

1. Chain topologies revisited

Consider, again, the network topology in Fig. 1. Recall that in Sec. III A we proved network synchronization in two subsequent steps. Specifically, we first proved that all network trajectories are globally exponentially convergent toward the polysynchronous subspace where $x_1 = x_4, x_2 = x_3$. We then showed that network dynamics reduced on such a subspace were globally exponentially convergent toward the synchronous subspace.

The subspaces $\mathcal{M}_2$ and $\mathcal{M}_1$ toward which convergence was proved were, in turn, determined by equivariance of network dynamics with respect to some permutation action. Notice that this equivariance property is a direct consequence of the fact that node 1 of the network is input equivalent to node 4 and node 2 is input equivalent to node 3. Moreover, the equivalent nodes of the two-nodes reduced network are also input equivalent.

VII. APPLICATIONS

A. Synchrony patterns for distributed computing

We now turn our attention to the problem of imposing some polysynchronous behavior for a network of interest. Specifically, we will impose different patterns of synchrony for a network composed of Hopfield models. The motivation that we have in mind here is that of multipurpose networks (i.e., networks that can be reused to perform different tasks). For example, this may be the case of sensor networks [40,41] where each polysynchronous steady state is associated to a specific set of inputs. A further notable example is the brain, where different polysynchronous behaviors are believed to play a key role in learning processes, for example (see, e.g., Ref. [42]).

We consider here a network of Hopfield models [43,44]

$$\dot{x}_i = -x_i + \sum_{j\in N_i} a_{ij}(t)h_{ij}(x_i,x_j,t) + u_i \tag{24}$$

where $a_{ij}(t)$ is the ith element of the time-varying interconnection matrix $A(t)$, h_{ij} represents the interconnection function from node j to node i, and u_i is an exogenous input to the ith node.

We start with the network in Fig. 4. Nodes denoted by the same shape are forced by the same exogenous input. Specifically: (i) $u_i(t) = 1 + \sin(0.7t)$ for the circle nodes; (ii) $u_i(t) = 5 + 3\sin(0.5t)$ for the square nodes; and (iii) $u_i(t) = 0$ for node 13.

Analogously, identical arrows denote identical coupling functions.

(i) the coupling between circle nodes is diffusive, bidirectional and linear: $h_{ij}(x_i,x_j,t) = a_{ij}(t)(x_j - x_i)$.

(ii) the coupling between square nodes is diffusive, unidirectional and linear.

(iii) the coupling between circle and square nodes is diffusive, bidirectional and nonlinear: $h_{ij}(x_i,x_j,t) = a_{ij}(t)[\arctan(x_j) - \arctan(x_j)]$.

(iv) the square nodes affect the dynamics of node 13 unidirectionally. Specifically, the dynamics of x_{13} is given by

$$\dot{x}_{13} = -x_{13} + (1 - b(t))\sum_{j=9}^{12} \frac{x_j}{1 + x_j} + b(t)\sum_{j=9}^{12} \frac{1}{1 + x_j} \tag{25}$$

where $b(t)$ is a parameter that is smoothly increased between 0 and 1. Notice that $b(t)$ can be used to switch between two different coupling functions.

We remark here that the input to node 13 is a well-known coupling mechanism in the literature on neural networks, and is termed as excitatory-only coupling (see, e.g., Ref. [45]).

It is straightforward to check that network dynamics are contracting (using, e.g., the matrix measure induced by the one-norm).

In Fig. 4 (right panel) the input-equivalent nodes are pointed out by means of colors: The associated linear polysynchronous subspace is

$$\mathcal{M}_1 = \{x_i = x_j, i,j = 1,\ldots,8\} \bigcap \bigcap \{x_i = x_j, i,j = 9,\ldots,12\}$$

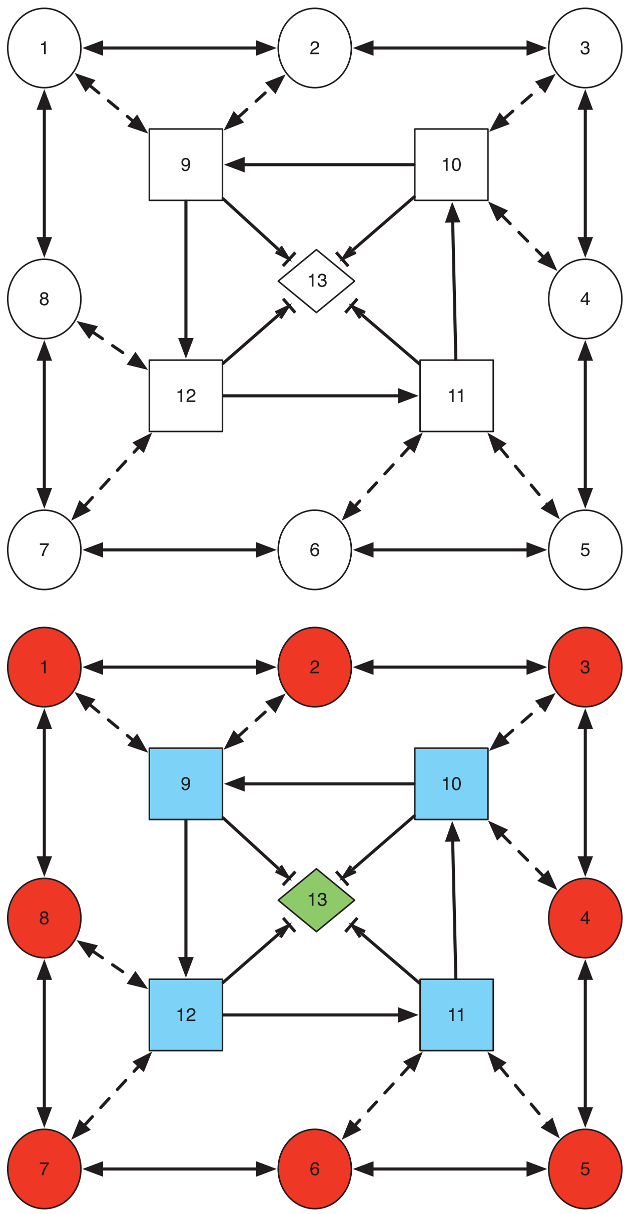

FIG. 4. (Color online) Network of Hopfield models used in Sec. VII A (top panel). The input-equivalent nodes are pointed out in the bottom panel.

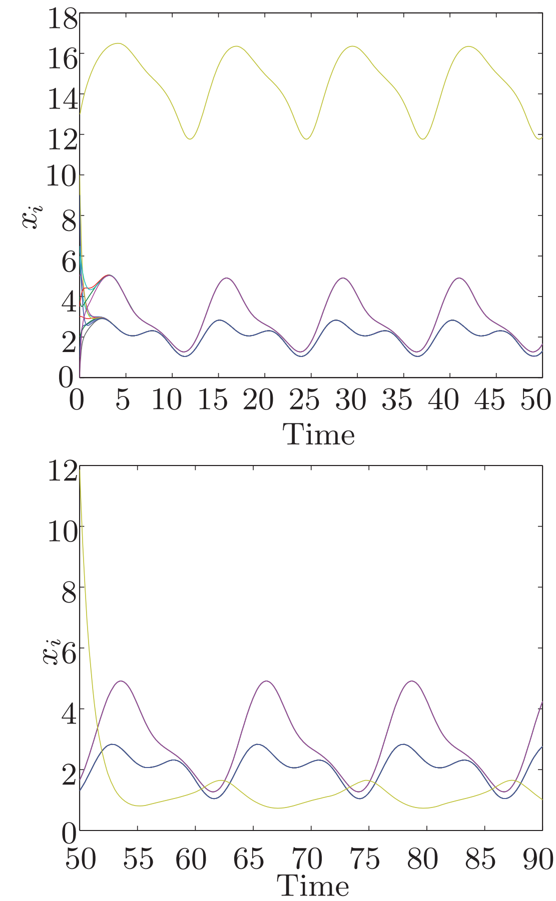

FIG. 5. (Color online) Network of Hopfield models Eq. (24) when (top panel) $b(t)$ in Eq. (25) is equal to 0. Notice the presence of three synchronized groups of nodes, corresponding the three classes of input-equivalent nodes pointed out in Fig. 4. The same synchronized groups are present when $b(t)$ in is switched to 0 (bottom panel). Notice that, in this case, the change of the coupling modifies the temporal behavior of node 13.

Furthermore, it is easy to check that $\mathcal{M}_1$ is flow invariant. Now, since network dynamics are contracting, all of its trajectories converge toward a unique solution embedded into $\mathcal{M}_1$. That is, at steady state all the nodes having the same color in Fig. 4 are synchronized. Figure 5 (left panel) clearly confirms the theoretical analysis, showing the presence of the three synchronized clusters, when $b(t) = 0$.

The same synchronized behavior is kept even when $b(t)$ smoothly varies from 0 to 1. Indeed, network dynamics is still contracting and the input-equivalence property defining $\mathcal{M}_1$ is preserved. In Fig. 5 (right panel) the behavior of the network is shown when at $t = 50$, $b(t)$ is set to 1.

Notice that the variation of $b(t)$ from 0 to 1 causes an inhibitory effect of the level of x_{13}. This is due to the fact that when $b(t) = 0$, x_{13} is forced by the sum of increasing sigmoidal functions. Conversely, when $b(t) = 1$, x_{13} is forced by the sum decreasing sigmoidal functions.

Now, assume that we need to create a synchronized cluster consisting of nodes 2, 4, 6, 8, for example. A way to achieve this task is that of modifying the input-equivalence property defining $\mathcal{M}_1$ and to impose an input-equivalence defining the subspace

$$\begin{aligned} \mathcal{M}_2 = \{x_i = x_j, i,j = 1,3,5,7\} \bigcap \\ \bigcap \{x_i = x_j, i,j = 2,4,6,8,\} \bigcap \\ \bigcap \{x_i = x_j, i,j = 9,\ldots,12\}. \end{aligned}$$

In turn, this can be done by smoothly varying the topology of the network (e.g., by diffusively coupling node 13 to the nodes 2, 4, 6, 8). The coupling function used to this aim, which preserves the contracting property, is

$$h_i(x_i,x_j) = h(x_j) - h(x_i), \qquad h(x) = \frac{1 - e^{-x}}{1 + e^{-x}}.$$

In Fig. 6 (left panel) this topology is shown, together with the class of input equivalence. The same figure (right panel)

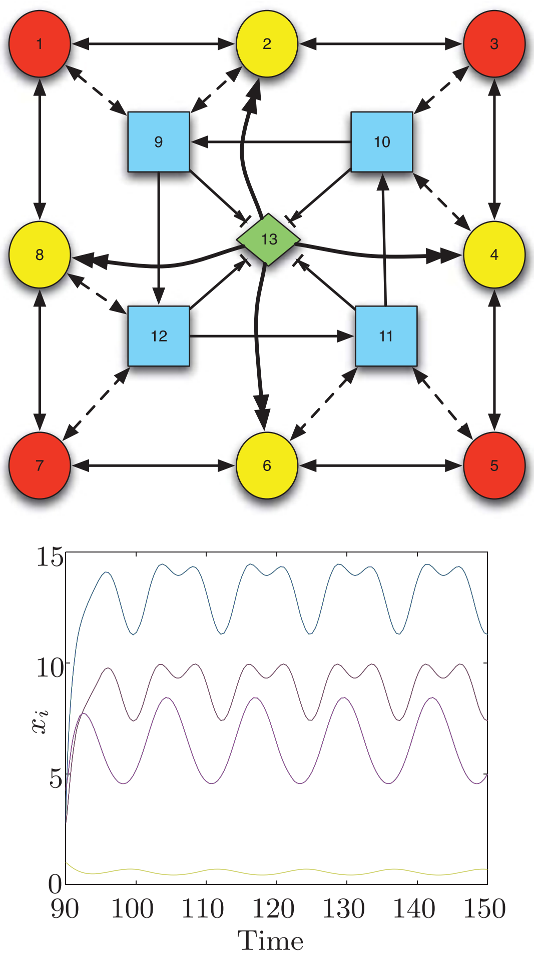

FIG. 6. (Color online) Network of Hopfield models used in Sec. VII A. Top panel: two links are activated by node 13, creating a class of input-equivalent nodes (in yellow). Bottom panel: temporal evolution of network nodes' dynamics. Notice the presence of a group of synchronized nodes, corresponding to the input-equivalence class.

shows the behavior of the network, pointing out that a cluster of synchronized nodes arises.

B. Chemotaxis with quorum

In the above examples, we assumed that each node of the network communicates directly with its neighbors. This assumption on the communication mode is often made in the literature on synchronization (see, e.g., [46–48] and references therein). In many natural systems, however, network nodes do not communicate directly, but rather by means of the environment. This mechanism, known as quorum sensing [49–51] is believed to play a key role in bacterial infection, as well as in bioluminescence and biofilm formation, for example [52,53]. Although to our knowledge this has not yet been studied experimentally, plausibly quorum sensing may also play a role in bacterial chemotaxis. Indeed, such a mechanism would enhance the robustness of the chemotactic response [54], with respect both to noise (including Brownian noise) and to the large variations in gene expressions between individual cells [55].

From a network dynamics viewpoint, a detailed model of such a mechanism would need to keep track of the temporal evolution of the environmental (shared) quantity, resulting in an additional set of ordinary differential equations [51,56]

$$\begin{aligned} \dot{x}_i &= f(x_i,z) \quad i = 1,\ldots,N \\ \dot{z} &= g(z,\Psi(X),t). \end{aligned} \tag{26}$$

In the above equation, N is the number of nodes sharing the same environment (medium). The set of state variables of the nodes is x_i, $X = [x_1^T,\ldots,x_N^T]^T$, while the set of the state variables of the common medium dynamics is z. Notice that the medium dynamics can be of different dimensions (e.g., $x_i \in \mathbb{R}^n$, $z \in \mathbb{R}^d$). The dynamics of the nodes affect the dynamics of the common medium by means of some coupling (or input) function, $\Psi: \mathbb{R}^{Nn} \to \mathbb{R}^d$. We assume that $\partial f/\partial z$ is bounded (that is, all of its elements are bounded).

In Ref. [51] it is shown that synchronization of Eq. (26) is attained if the reduced order virtual system

$$\dot{y} = f(y,y_z) \tag{27}$$

is contracting. Notice that the choice of such a reduced order virtual system is made possible by the fact that network Eq. (26) are symmetric with respect to any permutation of nodes state variables, x_i.

Consider, again, the chemotaxis model in Eq. (15) coupled by means of a quorum-sensing mechanism, with $\phi(u/x) = u/x$

$$\begin{aligned} \dot{x}_i &= x_i(y_i - 1) + h(y_i,z) \\ \epsilon\dot{y}_i &= \frac{u}{x_i} - y_i \\ \dot{z} &= g(z,\Psi(Y),t). \end{aligned} \tag{28}$$

In the above model subscript i is used to denote the state variables of the ith node and $Y = [y_1^T,\ldots,y_N^T]^T$. The ith node affects the dynamics of the shared variable, z, by means of y_i. Node-to-node communication is implemented by means of the input function h.

Notice that the presence of the coupling term and of the medium dynamics destroys the symmetry responsible of the invariance under input scaling. We are now interested in checking under what conditions invariance under input scaling is kept for a population the chemotaxis models in Eq. (28). We are motivated by the fact that, intuitively, bacteria go up a nutrient gradient toward the nutrient's source, with little interest for the absolute nutrient concentration.

We model the interaction between bacteria and the environment with a dimerization process

$$h(y_i,z) = K(y_i - 1)z.$$

Dimerization is a fundamental reaction in biochemical networks where two species combine to form a complex, as in the case of enzymes binding with substrates, for example [57].

In what follows, we use our results to show that a possible environmental model that ensures invariance under input scaling is

$$\dot{z} = -z - 1/N \sum_{i=1}^{N} x_i z.$$

That is, the model analyzed in the rest of this section is

$$\begin{aligned} \dot{x}_i &= x_i(y_i - 1) + K(y_i - 1)z \\ \epsilon \dot{y}_i &= \phi(u/x_i) - y_i \\ \dot{z} &= -z - 1/N \sum_{i=1}^{N} x_i z. \end{aligned} \tag{29}$$

We show that such a network preserves invariance under input scaling (i.e., such a behavior is not lost when nodes are coupled through the medium dynamics, z).

Since our aim is to explain the onset of a symmetric synchronous behavior for the network, we will consider a virtual system that embeds the dynamics of the common medium

$$\begin{aligned} \dot{y}_x &= y_x(y_y - 1) + K(y_y - 1)y_z \\ \epsilon \dot{y}_y &= \phi(u/y_x) - y_y \\ \dot{y}_z &= -y_z - 1/N \sum_{i=1}^{N}(x_i y_z). \end{aligned} \tag{30}$$

Notice that the above system represents a hierarchy (see Sec. II A) consisting of two subsystems: the (virtual) nodes dynamics $[y_x(t), y_y(t)]$, and the (virtual) medium dynamics, $z(t)$. Therefore, Eq. (30) is contracting if each of the subsystems is contracting (even in different metrics).

Now, it is straightforward to check that the dynamic of y_z is contracting. Thus, to complete the analysis, we have to check if the y dynamics is contracting. Similarly to the analysis of Sec. V B, we have

$$\ddot{y}_y^* + \frac{\dot{y}_y^*}{\epsilon} + \frac{1}{\epsilon}\left(\frac{u}{y_x} + \frac{uKy_z}{y_x^2}\right) y_y^* = 0, \tag{31}$$

where $y_y^* = y_y - 1$. That is, following exactly the same steps as those used in Sec. V B, we have that the above dynamics is contracting if

$$\frac{u}{y_x} + \frac{uKy_z}{y_x^2} < \frac{1}{2\epsilon}. \tag{32}$$

Notice that the above condition is satisfied if: (i) the concentration of y_x (and hence of x_i) is sufficiently high with respect to the concentration of y_z (and hence of z); (ii) its dynamics is sufficiently slow (ϵ small); and (iii) K is properly tuned. Recall from Sec. V B that both (i) and (ii) are true by hypotheses.

Thus, under the above conditions we have that the virtual system is contracting, and hence synchronization of network nodes is attained. Moreover, it is straightforward to check that the particular choice of the coupling function and of the medium dynamics ensures that all the hypotheses of Theorem 9 are satisfied with the actions

$$\begin{aligned} \gamma_i(y_{x,i}, y_{y,i}, y_z) &\rightarrow (y_{x,i}/u_{\min,i}, y_{y,i}, y_z/u_{\min,i}) \\ \rho_i u_i &\rightarrow u_i/u_{\min,i} \end{aligned} \tag{33}$$

where the subscripts i denote the system state variables and the actions associated to the input $u_i(t)$ (see Sec. V B for further details). This, in turn implies that the virtual system exhibits the invariance under input scaling. Now, recall that network nodes are particular solutions of the virtual system. Thus, all network nodes globally exponentially converge toward each other (since the virtual system is contracting), while exhibiting the invariance under input scaling (by virtue of Theorem 9).

C. Quorum with periodic inputs or communication delays

Quorum-sensing mechanisms exploit the symmetry of a dynamic system under permutation of individual elements. From a contraction point of view, this allows one to use a virtual system of the same dimension as individual elements, and such that each individual trajectory represents a particular solution of the virtual system.

This principle extends straightforwardly to two cases of practical interest. The first is the case when the environment or the entire system is also subject to an external periodic input, thus yielding a spatiotemporal symmetry. The second case is when communications between nodes and the environment exhibit significant delays. This case may model actual delays in information transmission (e.g., in a natural or robotic swarm application) and signal processing, or for instance the effect of diffusion or of nonhomogeneous concentrations in a biochemical context.

We now show that the combined use of symmetries and contraction analysis can be used to provide a sufficient condition to control the periodicity of the synchronous final behavior of a quorum sensing of interest. The idea is to force a network of interest by means of a periodic input, $r(t)$, and then to provide conditions ensuring that the network becomes synchronized onto a periodic orbit having the same period as $r(t)$. See the companion paper [51] for further details. Our main result is as follows.

Theorem 12. Consider the following network

$$\begin{aligned} \dot{x}_i &= \tilde{f}(x_i, z) \quad i = 1, \ldots, N \\ \dot{z} &= \tilde{g}(z, \Psi(x_1, \ldots, x_N)) + r(t) \end{aligned} \tag{34}$$

where $r(t)$ is a T-periodic signal. All the nodes of the network synchronize onto a periodic orbit of period T, say $x_T(t)$, if: (i) $f(x_i, v(t))$ is a contracting function; (ii) the reduced order system ($x_c(t) \in \mathbb{R}^n$)

$$\begin{aligned} \dot{x}_c &= f(x_c, z) \\ \dot{z} &= g(z, \Psi(x_c, \ldots, x_c)) + r(t) \end{aligned}$$

is contracting. Note that the dynamics $\tilde{f}$ and $\tilde{g}$ include the coupling terms between nodes and environment.

Proof. Consider the virtual system

$$\dot{y}_1 = f(y_1, z). \tag{35}$$

By hypotheses Eq. (35) is contracting and hence the nodes state variables will converge toward each other (i.e., $|x_i - x_j| \rightarrow 0$ as $t \rightarrow +\infty$). That is, all the network trajectories converge toward a unique common solution, say $x_c(t)$. This in turn implies that, after transient, network dynamics are described by the reduced order system

$$\begin{aligned} \dot{x}_c &= f(x_c, z) \\ \dot{z} &= g(z, \Psi(x_c, \ldots, x_c)) + r(t). \end{aligned}$$

Now, the above system is contracting by hypotheses and $r(t)$ is a T-periodic signal. In turn, this implies that all of its solutions will converge toward a unique T-periodic solution, i.e.,

$$|x_c(t) - x_T(t)| \rightarrow 0, \quad t \rightarrow +\infty.$$

This proves the result. ■

Notice that the proof of the above result is based on the combined use of symmetries and contraction. Specifically, the use of a reduced order virtual system is made possible by the fact that the network is symmetric with respect to any permutation of the nodes' state variables. Moreover, contraction analysis provides sufficient conditions guaranteeing that all the solutions of the virtual system converge to a periodic trajectory having the same period as the input, $r(t)$. Since the nodes' state variables are particular solutions of the virtual system, this implies that network nodes are synchronized onto a periodic orbit having the same period of $r(t)$.

The case when some form of delay occurs in the communication can be treated similarly, by using results on the effect of delays in contracting systems [58]. Consider for instance a network of linearly diffusively coupled nodes x_i coupled by means of a quorum-sensing mechanism

$$\begin{aligned} \dot{x}_i &= f(x_i) + K_{iz}[z(t - T_{zx}) - x_i(t)] \\ \dot{z} &= g(z) + \frac{1}{N}\sum K_{zi}[x_i(t - T_{xz}) - z(t)], \end{aligned} \tag{36}$$

where $f(\cdot)$ and $g(\cdot)$ (denoting the intrinsic dynamics of the network nodes and of the common medium) are contracting within the same metric, the constant $T_{zx} \geqslant 0$ represents a communication or computation delay from the medium to the nodes, and similarly the constant $T_{xz} \geqslant 0$ represents a delay from the nodes to the medium.

Notice that network Eq. (36) is symmetric with respect to any permutation of the nodes' state variables. As discussed above, this symmetry implies that the network can be analyzed by using the reduced order virtual system

$$\begin{aligned} \dot{y}_x &= f(y_x) + K_{iz}[y_z(t - T_{zx}) - y_x(t)] \\ \dot{y}_z &= g(y_z) + \frac{1}{N}\sum K_{zi}[y_x(t - T_{xz}) - y_z(t)]. \end{aligned} \tag{37}$$

As proven in Ref. [58], all the trajectories of the above system converge toward each other if $f(\cdot)$ and $g(\cdot)$ are contracting within the same metric. Since the nodes' state variables are particular solutions of the virtual system Eq. (37), it follows that all the solutions of the network converge toward a fixed point in the network phase space. Now, as shown in Ref. [58], if $K_{iz} = \frac{1}{N}K_{zi}$, then $z(t)$ tends to the fixed value $\bar{z}$ and all nodes tend to the common equilibrium value $x_i = x_j = \bar{x}$, $\forall i,j$. Moreover, $\bar{x}$ and $\bar{y}$ are such that

$$\begin{aligned} f(\bar{x}) + k_{iz}(\bar{z} - \bar{x}) &= 0 \\ g(\bar{z}) + k_{iz}(\bar{x} - \bar{z}) &= 0. \end{aligned}$$

VIII. CONCLUSION

We presented a framework for analyzing and/or controlling stability of dynamical systems by using a combination of structural properties of the system's vector field (symmetries) and convergence properties (contraction). We first showed that the symmetries of a contracting vector field are transferred to its solutions, and then generalized this result by using virtual systems. In turn, those results were used to describe invariance under input scaling in transcriptional systems, a property believed to play a key role in many sensory systems. The case of a quorum-sensing network with delays was also considered. Finally, we showed how our results could suggest a mechanism for quorum sensing in bacterial chemotaxis, thus combining symmetries in cell interactions with invariance to input scaling.

ACKNOWLEDGMENTS

The authors would like to thank Professor Marty Golubitsky for many insightful comments and suggestions.

[1] M. Golubitsky and I. Stewart, *The Symmetry Perspective: from Equilibrium to Chaos in Phase Space and Physical Space* (Birkhäuser, Berlin, 2003).
[2] J. Marsden and T. Ratiu, *Introduction to Mechanics and Symmetry* (Springer-Verlag, New York, 1994).
[3] P. Oliver, *Applications of Lie Groups to Mechanics and Symmetry* (Springer-Verlag, Berlin, 1986).
[4] P. G. Mehta, G. Hagen, and A. Banaszuk, SIAM J. Appl. Dyn. Syst. **6**, 549 (2007).
[5] S. Bonnabel, P. Martin, and P. Rouchon, IEEE Transactions on Automatic Control **54**, 1709 (2009).
[6] M. Spong and F. Bullo, IEEE Transactions on Automatic Control **50**, 1025 (2005).
[7] W. Koon and J. Marsden, SIAM J. Control Optim. **35**, 901 (1997).
[8] Q. C. Pham and J. J. E. Slotine, Neural Networks **20**, 62 (2007).
[9] L. Gerard and J. Slotine, e-print arXiv:q-bio/0612049.
[10] M. Golubitsky, I. Stewart, and A. Torok, SIAM J. Appl. Dyn. Syst. **4**, 78 (2005).
[11] M. Golubitsky and I. Stewart, Bulletin of the American Journal of Mathematics **43**, 305 (2006).
[12] I. Stewart, M. Golubitsky, and M. Pivato, SIAM J. Appl. Dyn. Syst. **2**, 609 (2003).
[13] Y. A. Kuznetsov, *Elements of Applied Bifurcation Theory* (Springer-Verlag, New York, 2004).
[14] W. Lohmiller and J. J. E. Slotine, Automatica **34**, 683 (1998).
[15] W. Wang and J. J. E. Slotine, Biol. Cybern. **92**, 38 (2005).
[16] P. Hartman, Canadian J. Math. **13**, 480 (1961).
[17] D. C. Lewis, Am. J. Math. **71**, 294 (1949).
[18] G. Dahlquist, *Stability and Error Bounds in the Numerical Integration of Ordinary Differential Equations* (Transactions of the Royal Institute of Technology, Stockholm, 1959).
[19] S. M. Lozinskii, Izv. Vtssh. Uchebn. Zaved Matematika **5**, 222 (1959).
[20] J. Slotine, International Journal of Adaptive Control and Signal Processing **17**, 397 (2003).
[21] S. Mallat, *Proceedings of European Signal Processing Conference (EUSIPCO)* (2010).

[22] I. Epstein and M. M. Golubitsky, Chaos **3**, 1 (1993).
[23] M. Arcak, e-print arXiv:0908.2614.
[24] P. Freund, *Introduction to Supersymmetry* (Cambridge University Press, Cambridge, 1988).
[25] L. H. Ryder, *Quantum Field Theory*, 2nd ed. (Cambridge University Press, Cambridge, 1996).
[26] L. Goentoro, O. Shoval, M. Kirschner, and U. Alon, Mol. Cell **36**, 894 (2009).
[27] O. Shoval, L. Goentoro, Y. Hart, A. Mayo, E. Sontag, and U. Alon, Proc. Natl. Acad. Sci. **107**, 15995 (2010).
[28] L. Goentoro and M. Kirschner, Mol. Cell **36**, 872 (2009).
[29] C. Cohen-Saidon, A. Cohen, A. Sigal, Y. Liron, and U. Alon, Mol. Cell **36**, 885 (2009).
[30] P. Eichenberger, M. Fujita, S. Jensen, E. Conlon, D. Rudner, S. Wang, C. Ferguson, K. Haga, T. Sato, J. Liu, and R. Losick, PLoS Bio. **2**, e328 (2004).
[31] R. Milo, S. Shen-Orr, S. Itzkovitz, N. Kashtan, D. Chklovskii, and U. Alon, Science **298**, 824 (2002).
[32] S. Mangan, S. Itzkovitz, N. Kashtan, D. Chklovskii, and U. Alon, J. Mol. Biol. **356**, 1073 (2006).
[33] D. Kim, Y. Kwon, and K. Cho, Bioessays **30**, 1204 (2008).
[34] A. Celani and M. Vergassola, Proc. Natl. Acad. Sci. USA **107**, 1391 (2010).
[35] Y. Tu, T. Shimizu, and H. Berg, Proc. Natl. Acad. Sci. USA **105**, 14855 (2008).
[36] W. Lohmiller and J. Slotine, e-print arXiv:nlin/0510025.
[37] E. Montbrió, J. Kurths, and B. Blasius, Phys. Rev. E **70**, 056125 (2004).
[38] E. Oh, K. Rho, H. Hong, and B. Kahng, Phys. Rev. E **72**, 047101 (2005).
[39] F. Sorrentino and E. Ott, Phys. Rev. E **76**, 056114 (2007).
[40] G. Martinelli, Neural Processing Letters **27**, 277 (2008).
[41] M. Yarvis, N. Kushalnagar, H. Singh, A. Rangarajan, Y. Liu, and S. Singh, in *IEEE InfoCom* (2005).
[42] E. M. Izhikevich, *Dynamical Systems in Neuroscience: The Geometry of Excitability and Bursting* (MIT Press, Cambridge, 2006).
[43] J. Hopfield, Proc. Natl. Acad. Sci. USA **79**, 2554 (1982).
[44] H. Oshima and T. Odagaki, Phys. Rev. E **76**, 36114 (2007).
[45] J. E. Rubin, Phys. Rev. E **74**, 021917 (2006).
[46] M. E. Newman, SIAM Rev. **45**, 167 (2003).
[47] S. Boccaletti, V. Latora, Y. Moreno, M. Chavez, and D. Hwang, Phys. Rep. **424**, 175 (2006).
[48] T. Danino, O. Mondragon-Palomino, L. Tsimring, and J. Hasty, Nature (London) **463**, 326 (2010).
[49] M. Miller and B. Bassler, Annu. Rev. Microbiol. **55**, 165 (2001).
[50] C. Nardelli, B. Bassler, and S. Levin, J. Biol. **7**, 27 (2008).
[51] G. Russo and J. Slotine, Phys. Rev. E **82**, 041919 (2010).
[52] C. Anetzberger, T. Pirch, and K. Jung, Mol. Microbiol. **2**, 267 (2009).
[53] C. D. Nadell, J. Xavier, S. A. Levin, and K. R. Foster, PLoS Comput. Bio. **6**, e14 (2008).
[54] N. Tabareau, J. Slotine, and Q. Pham, PLoS Comput. Bio. **6**, e1000637 (2010).
[55] S. Tyagu, Science **329**, 518 (2010).
[56] G. Katriel, Physica D **237**, 2933 (2008).
[57] Z. Szallasi, J. Stelling, and V. Periwal, *System Modeling in Cellular Biology: From Concepts to Nuts and Bolts* (MIT Press, Cambridge, 2006).
[58] W. Wang and J. Slotine, IEEE Transactions on Automatic Control **51**, 712 (2006).